Distribution Agreement

In presenting this thesis as a partial fulfillment of the requirements for a degree from Emory University, I hereby grant to Emory University and its agents the non-exclusive license to archive, make accessible, and display my thesis in whole or in part in all forms of media, now or hereafter now, including display on the World Wide Web. I understand that I may select some access restrictions as part of the online submission of this thesis. I retain all ownership rights to the copyright of the thesis. I also retain the right to use in future works (such as articles or books) all or part of this thesis.

Anna Eligulashvili April 12, 2022

Progress Towards Visualizing Single Molecules for Transcription Studies

by

Anna Eligulashvili

Dr. Laura Finzi
Adviser

Department of Physics

Dr. Laura Finzi

Adviser

Dr. Eladio Abreu

Committee Member

Dr. Daniel Weissman

Committee Member

2022

Progress Towards Visualizing Single Molecules for Transcription Studies

By

Anna Eligulashvili

Dr. Laura Finzi

Adviser

An abstract of
a thesis submitted to the Faculty of Emory College of Arts and Sciences
of Emory University in partial fulfillment
of the requirements of the degree of
Bachelor of Science with Honors

Department of Physics

2022

Abstract

Progress Towards Visualizing Single Molecules for Transcription Studies

By Anna Eligulashvili

Deoxyribonucleic acid (DNA) is a complex biomolecule that serves as the universal genetic code and codes for all processes necessary for life. The first step in the expression of this genetic code is transcription, which is carried out by the ribonucleic acid polymerase (RNAP), a DNA-binding protein. In order to gain more insight on RNAP functional irregularities such as roadblocking and backtracking, various methods were explored for using the correlative optical trap (C-Trap) to obtain force, distance, and fluorescence data as a function of time. Using the high-resolution dual optical tweezers and multi-laser confocal microscopy system in the C-Trap, force-extension curves and kymographs were collected and analyzed for a variety of DNA tethers and fluorophores. Initial experiments aimed at visualizing the full length of a 14 kbp tether with SYBR Green DNA-intercalating dye. This experiment required high force to cause intercalation and molecules often ruptured. Other experiments were conducted with a 12 kbp DNA tether that was sparsely labeled with Cy5 fluorophores. While some data were promising, the resolution and lifetimes of the fluorophores were too low to be suitable in future transcription experiments. This drawback led to the use of an oxygen scavenger system consisting of a Glucose-Catalase-Oxidase oxygen scavenger and Trolox, a radical-reducing reagent, which together significantly increased the probability of DNA tethering and the lifetime of the fluorescent signal. In addition to visualizing DNA tethers, fluorescent experiments also confirmed the possibility of using labeled biotinylated RNAP labeled with Cy3-labeled streptavidin proteins to track RNAP movement along a tether. Preliminary experiments with RNAP showed specific binding of the enzyme to promoter regions, translocation, and disassociation. All fluorescent experiments were optimized by altering the concentrations of chemical reagents, employing oxygen scavenging methods, and adjusting the focus and filters of the confocal detectors. These aforementioned experiments show that the C-Trap can be used for such transcription experiments and provide protocols optimize the results.

Progress Towards Visualizing Single Molecules for Transcription Studies

By

Anna Eligulashvili

Dr. Laura Finzi

Adviser

A thesis submitted to the Faculty of Emory College of Arts and Sciences
of Emory University in partial fulfillment
of the requirements of the degree of
Bachelor of Science with Honors

Department of Physics

2022

Acknowledgements

Foremost, I would like to express my deep and sincere gratitude to Dr. Laura Finzi and Dr. David Dunlap for their mentorship and support throughout my thesis. I would also like to thank Dr. Yue Lu for his time, guidance, and assistance with the benchwork and experiments. Additionally, thank you to my committee members Dr. Eladio Abreu and Dr. Daniel Weissman for their support leading up to my defense. I would also like to express my thanks to Susan Cook for her help coordinating my undergraduate work within the Department of Physics, and to Jin Qian, Dylan Collette, and Allison Cartee for their continued encouragement. Lastly, I would like to acknowledge Dr. Irina Artsimovitch for contributing biotinylated RNA polymerase.

Table of Contents

List of Figures

1 Introduction

2 The C-Trap Microscope

3 Materials and Methods

4 Results and Analysis

1 Introduction

1.1 DNA as a Key Construct to Life

Deoxyribonucleic acid (DNA) is a complex, double-stranded biological polymer that serves as a universal genetic template to all living organisms[1]. The primary structure of DNA consists of nucleotide monomers connected by phosphodiester bonds to form a sugar-phosphate backbone (Fig. 1A); these nucleotides then hydrogen bond with the complementary chain to form a double-helical structure. This complex tertiary structure consists of two phosphodiester backbones on the exterior with hydrogen-bonded nucleotides on the interior[2] (Fig. 1B).

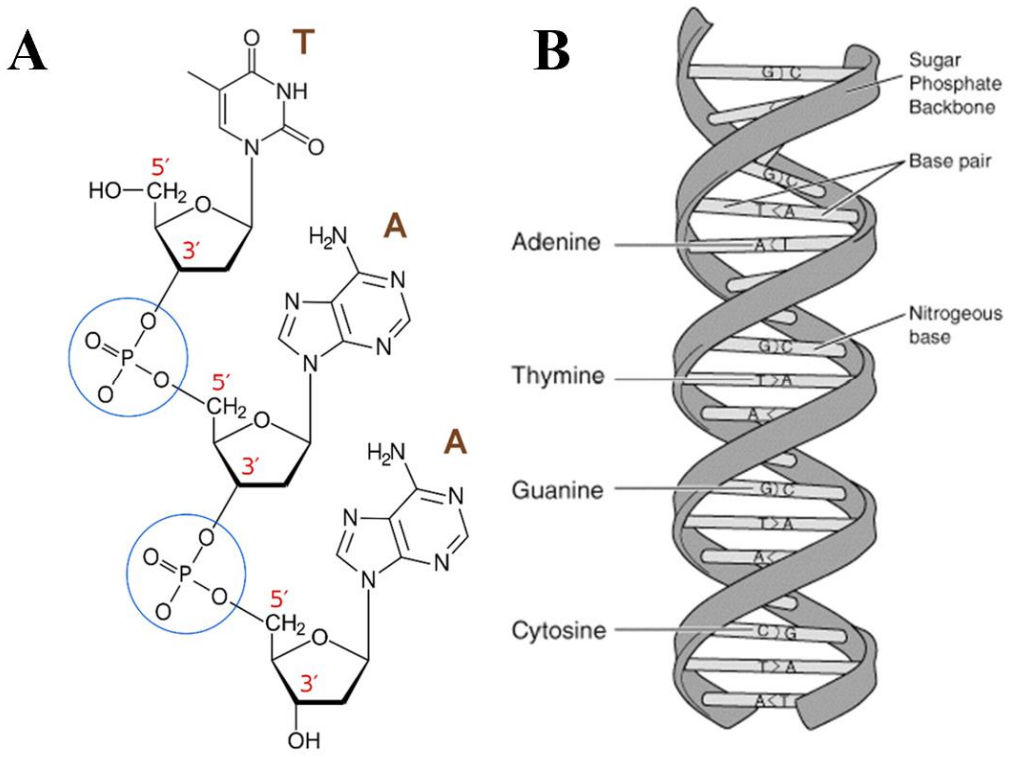

Figure 1. (A) Two phosphodiester bonds between successive nucleotides in a DNA strand[3]. **(B)** Tertiary structure of the DNA, showing the double-helix composed of the phosphodiester backbone and paired nucleotides[4].

The four characteristic monomers, or nucleotides, of DNA are adenine (A), cytosine (C), guanine (G), and thymine (T); though a given nucleotide can form a phosphodiester bond with any other nucleotide, hydrogen bonding between DNA strands can only occur between adenine and thymine or cytosine and guanine according to Watson-Crick base pairing rules[5] (Fig. 2).

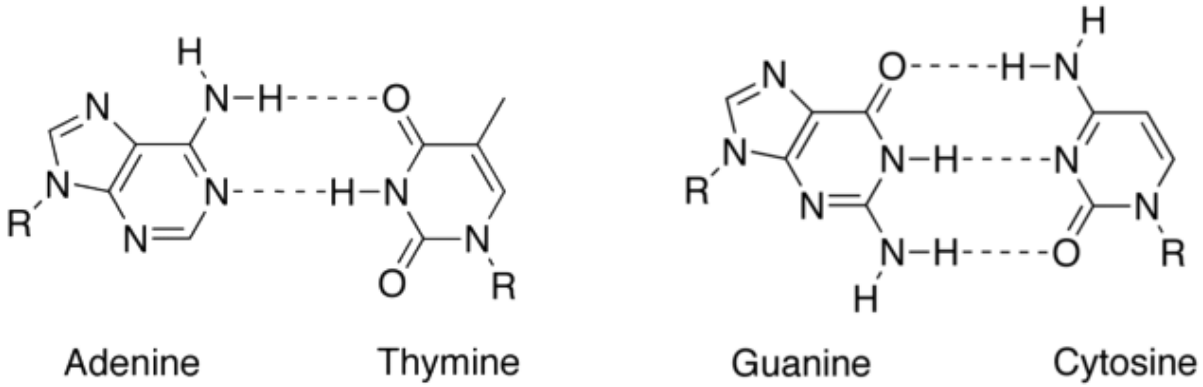

Figure 2. The chemical structures and bonds of the Watson-Crick nucleotide base pairs[6]. Adenine forms two hydrogen bonds with thymine (on the left) and guanine forms three hydrogen bonds with cytosine (on the right).

DNA serves as a key construct to life because it encodes for all biological processes that occur in living organisms. While the molecule itself may not be a catalyst, its transcription to RNA, followed by translation to protein, allows the genetic information to be utilized[7]. Expression of genes within DNA is regulated to maintain homeostasis[8].

1.2 DNA Mechanics

DNA mechanics significantly impacts replication and transcription, both on micro- and macro-scale levels, and is of interest in many scientific fields. Extensive research has helped reveal more information about DNA persistence length, topology, and supercoiling properties such as

twisting and bending stiffness. DNA interactions between the two strands, as well as with DNA-binding proteins, have also been studied in detail[9].

DNA has an iconic double-helical structure. Further research into DNA mechanics have revealed the interesting that this semiflexible polymer twists, bends, stretches, and supercoils under various environmental and experimental conditions. When the tertiary structure of DNA changes, its interactions with DNA-binding proteins change and impact cellular processes as well[9].

While some of these characteristics are outside the scope of this thesis, DNA's ability to stretch, compress, and bend are of particular interest for this thesis. *In vivo*, thermal fluctuations in the DNA's environment can create forces on the molecule that bend and twist the rigid molecule. *In vitro* experiments can model the effect of these forces on the DNA polymer by considering the biomolecule to be semiflexible and of fixed contour length exposed to compacting entropic forces that reduce the overall end-to-end extension[9,10]. Studies have shown that the extension of DNA molecules will vary linearly with force in the low-force condition, however at higher forces the extension will vary asymptotically[9]. The findings of these studies can be modeled with statistical mechanics and represented in force-extension diagrams (Fig. 3). This worm-like chain model assumes that a single DNA strand of a fixed contour length will have variations in persistence length when force is applied to stretch or compress the tether. Though this model begins to diverge from collected data at high forces due to unaccounted DNA elasticity and volume interactions, its accuracy at forces up to 70 pN makes it a sufficient model in experimental applications[11].

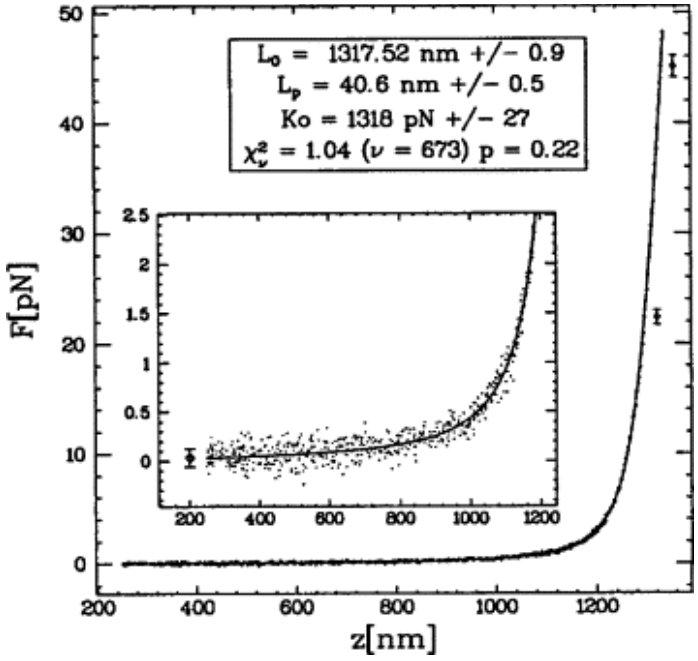

Figure 3. Characteristic force-extension curve of a single DNA[12].

1.3 RNA Polymerase and Transcription

Among the aforementioned DNA-binding proteins is ribonucleic acid polymerase (RNAP), which is a molecular motor that generates RNA molecules from the DNA template strand[13]. This RNA molecule is later used in translation as a blueprint for protein synthesis, making transcription an important step in the expression of the genetic code in DNA[7]. This stepwise process to expressing DNA is known as the Central Dogma of Molecular Biology (Fig. 4).

Figure 4. The Central Dogma of Molecular Biology depicting the steps in the expression of the genetic code[7].

The three steps of transcription are initiation, elongation, and termination[14] (Fig. 5).

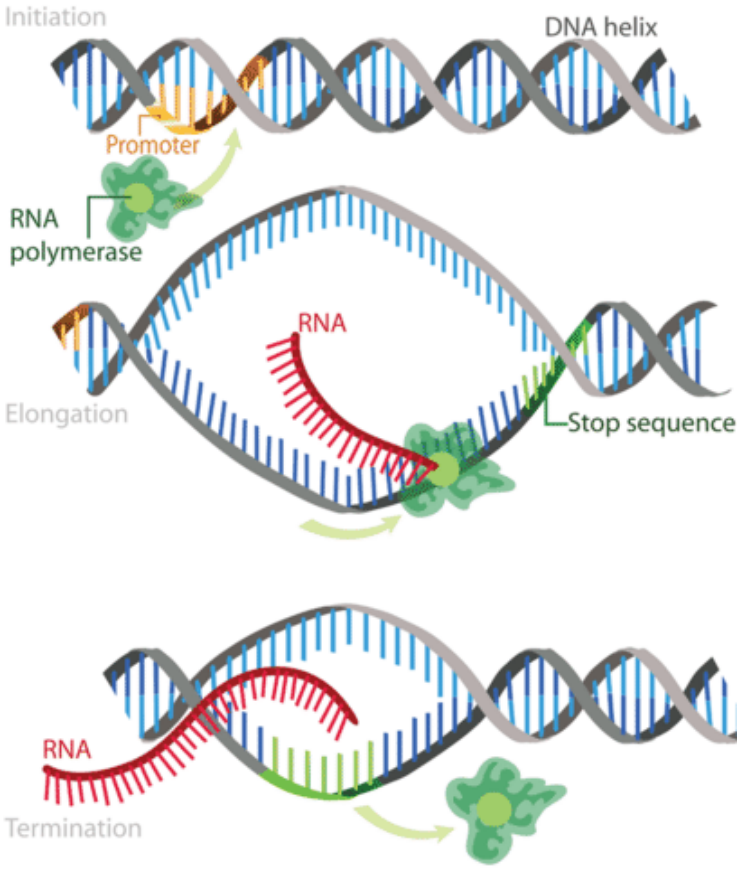

Figure 5. Schematic diagram representing the three steps of RNA transcription from a DNA template. From top to bottom, the steps are initiation, elongation, and termination[14].

To initiate, the RNAP must bind to the promoter sequence on the template strand of the DNA. This preliminary binding step progresses to separation of the double-stranded DNA (dsDNA) downstream, after which the RNAP can add nucleotides to a nascent RNA strand in a process called elongation. In this process, the complementary nucleotides are to a growing RNA that has opposite 5'-to-3' polarity of the template DNA strand. Base-pairing occurs in accordance with

the Watson-Crick rules with the exception of adenine, which binds to the nucleotide uracil (U) in RNA instead of thymine[14] (Fig. 6).

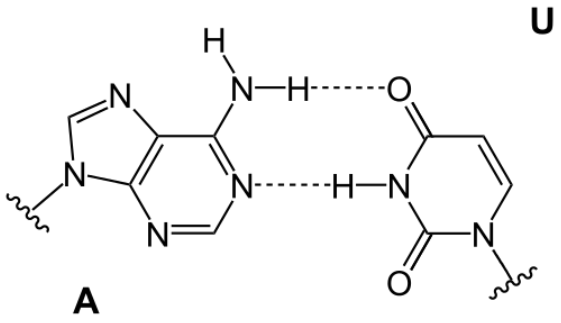

Figure 6. Chemical structure depicting the interaction between an adenine nucleotide (left) and uracil nucleotide (right), connected by two hydrogen bonds[15].

As RNAP moves along the template strand, it will reach a termination sequence that signals the end of transcription. Here, the RNAP will detach from the dsDNA and the completed RNA transcript will proceed to undergo post-transcriptional modifications before translation[16].

While polymerization catalyzed by RNAP is straight-forward, research has revealed that RNAP does not always follow the start and stop signals as expected; RNAP can stall at transcriptional roadblocks, introduce errors through slippage[17], and uncoupled translocation[18]. These behaviors are still being investigated and create many questions as to how DNA expression is regulated and what irregularities result.

1.4 Research Motivation

As indicated in the previous sections, the transcription of DNA is a key regulatory step. Given RNAP's crucial role this process, we must understand in detail how it works. To better understand these RNAP mechanisms, we must study exactly how RNAP behaves in varying

environmental and chemical conditions *in vitro.* Single molecule techniques can be used to monitor transcription in real-time in well controlled conditions. While other researchers have begun to study these behaviors with other techniques, exploration of RNAP movement using live force data and fluorescent visualization will furnish a more complete and accurate understanding of the transcription by RNAP.

1.5 Single Molecule Techniques in Biophysics

The foundation of this thesis arises from published RNAP work stemming from well-known single-molecule techniques, or experimental methods that aim to acquire data on one molecule at a time in contrast to measuring and analyzing averaged outcomes from a multitude of molecules[19]. To acquire force data on single molecules, common techniques include optical tweezers, magnetic tweezers (permanent or electromagnetic), and tethered particle motion[20]. Single-molecule data may also be obtained through fluorescence-based techniques such as confocal[20,21] or total internal reflection microscopy[22].

These two fluorescent techniques are dependent on the use of fluorescent molecules, such as DNA-intercalating dyes and cyanine dyes. While Cy dyes may be used to label biomolecules such as DNA and proteins, DNA-intercalating dyes such as SYBR Green have intrinsic affinity for DNA. These dyes are small molecules that will reversibly bind in between two nucleotide base pairs and may exhibit higher affinity when the DNA is stretched (Fig. 7). While these dyes allow visualization of the entire DNA molecule, they are known to decrease the stability of the DNA that may break especially under tension or perturbations[23].

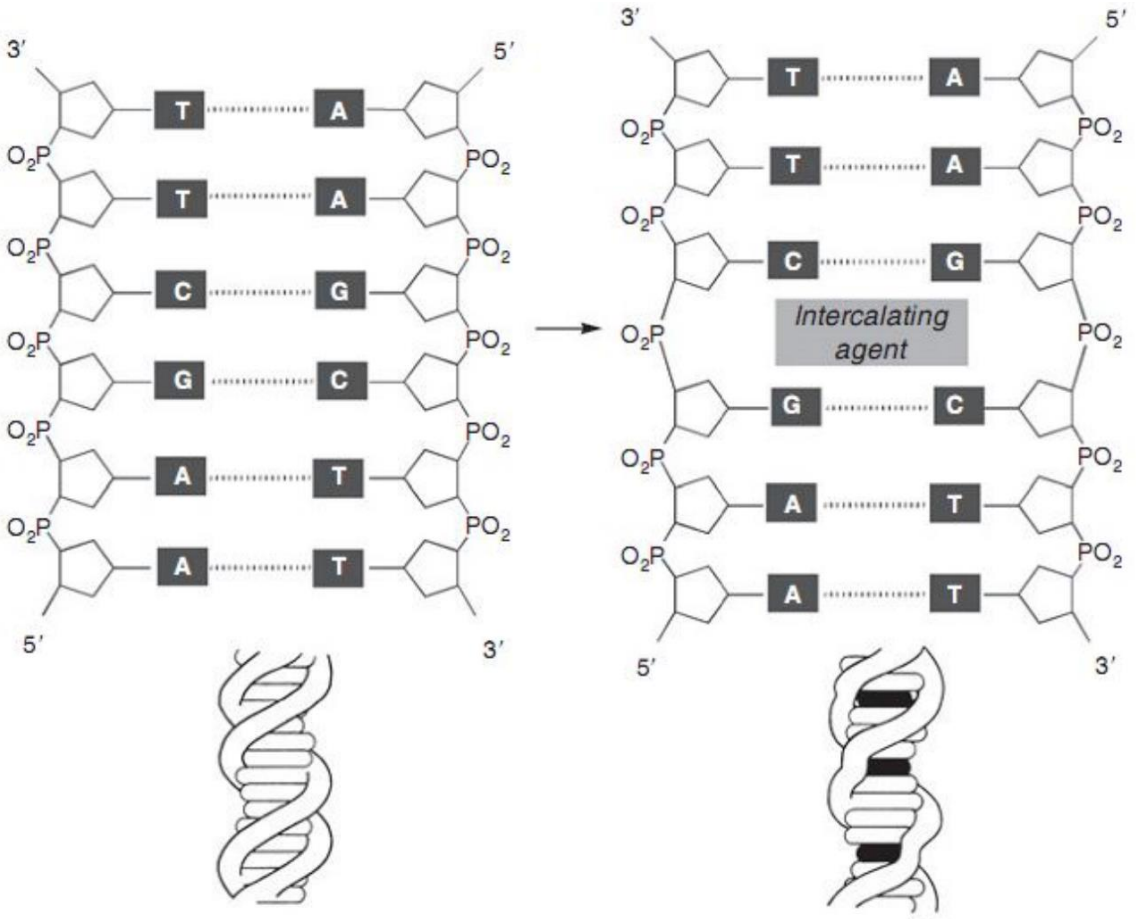

Figure 7. Mechanism of action of DNA-intercalating dyes[24]. The DNA molecule on the left does not contain the dye, and the DNA molecule on the right contains a DNA-intercalator in between base pairs.

In addition to DNA-intercalating dyes, fluorophores may instead be complexed to biomolecules to visualize a specific region or protein of interest in the sample. Cyanine (Cy) dyes, for example, can be incorporated on nucleotides or complexed to proteins (Fig. 8). Known for their photostability and enhanced water solubility, these dyes are superior to some previously dyes and are useful in experiments that require extended observations of fluorescence, such as transcription experiments[25].

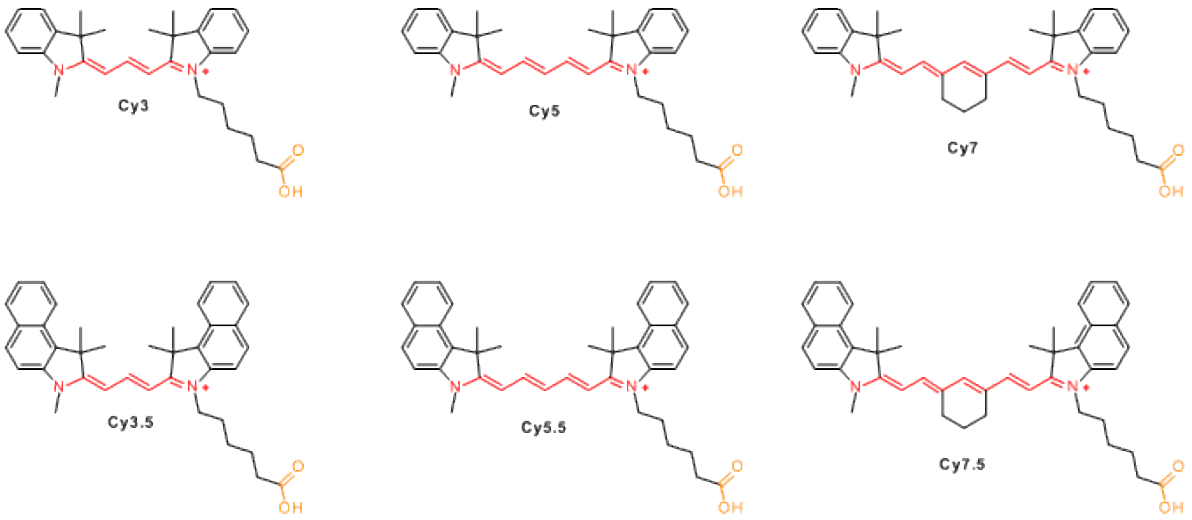

Figure 8. Chemical structures of commonly used Cy dyes, all of which contain two aromatic units connected with a polyalkene bridge and indole heterocyclic nuclei[26].

Regardless of the type of fluorophore used, confocal microscopy and confocal line microscopy are widely used methods in visualization of these fluorescent signals. While full-field confocal microscopy techniques collect photon data consecutively from single points along a raster pattern[27], line-scanning confocal microscopy repeatedly collects photon data along a single line[28]. Regardless of the extent of data collection method, the basic scientific principle of confocal microscopy is that the fluorophores are excited by a laser of a certain wavelength, and in their return to the ground state they emit photons that are detected by photon-counters[29] (Fig. 9). The photon data is then processed to compose an image in which higher photon counts are brighter.

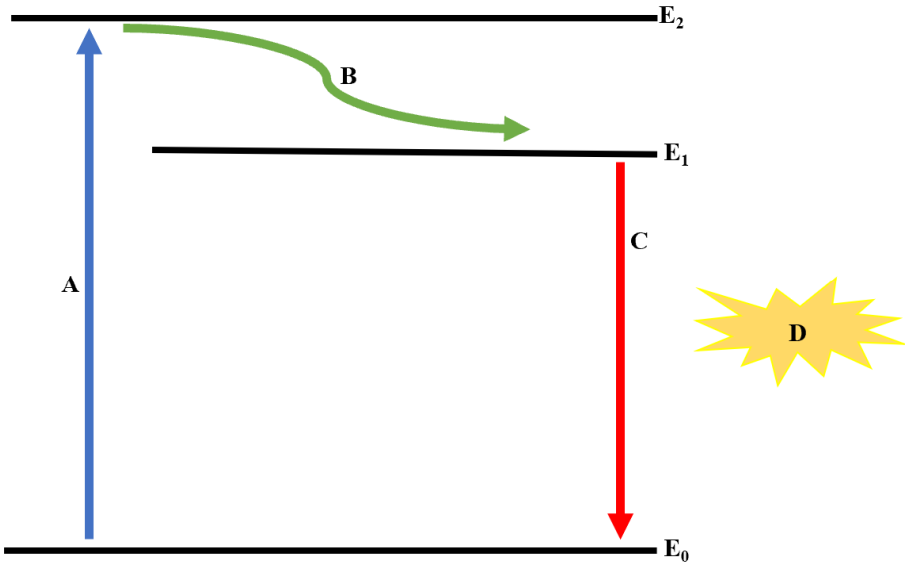

Figure 9. Schematic diagram representing the steps leading to photon emission[29]. After a molecule absorbs a high-energy photon emitted from the laser **(A)**, some energy is internally lost to the system **(B)**, after which the molecule returns to the ground state **(C)** and emits a low-energy photon to create a fluorescent signal **(D)**.

When information from force-based and fluorescent-based measurements is combined, a fuller picture of the biological mechanism or molecule of interest is obtained because components generating force and translocation in the process can be monitored. Specifically collecting information about one-molecule at a time allows for a sophisticated analysis of single-molecule behaviors, such as RNAP backtracking during transcription.

2 The C-Trap Microscope

2.1 Background

While optical tweezers and confocal microscopy have been used extensively since their development in 1986 and 1957, respectively, the C-Trap is a unique instrument that allows simultaneous use of these two techniques and obtain real-time data[25,30,31]. The machine consists

of a fixed flow cell, two trapping lasers that function as high-resolution dual optical tweezers, and three confocal lasers for confocal microscopy. The trapping lasers capture and record the position of beads, while the confocal lasers are turned on and off to excite fluorescent molecules. This all-in-one experimental setup allows for real-time data collection that encompasses information about the position of beads, force applied to the beads, and photon counts all as a function of time[31]. In addition, the C-Trap instrument leverages microfluidics for easy sample preparation.

2.2 Microfluidics

When preparing the C-Trap for an experiment, various solutions are loaded into syringes each leading into separate channels in the flow cell. Because these channels are separated by laminar flow instead of physical barriers, it is possible to capture beads in the optical traps and move them between channels (Fig. 10). The speed of the flow is controlled by a stable passive-pressure system control on the user interface and allows for selected channels to be opened and closed without displacing any solution or interfering with experimental measurements[31]. This no-barrier channel system becomes particularly useful when the traps need to capture beads from different channels or when a DNA tether has to be briefly dipped in fluorescent dye.

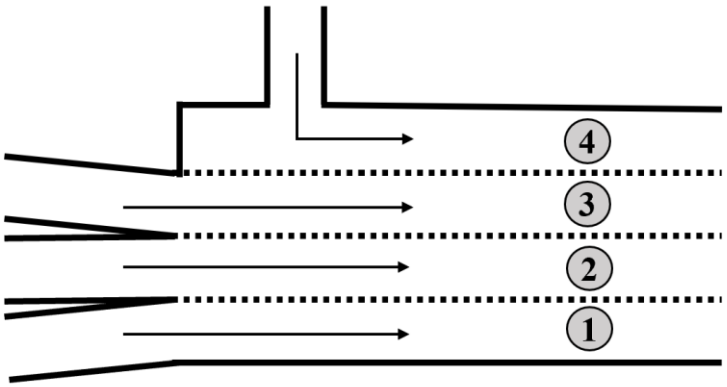

Figure 10. Schematic diagram of the different channels in the Lumicks flow cell.

2.3 Optical Tweezers

In the main body of the C-Trap machine are located two high-resolution optical tweezers that are used to capture beads or cells (Fig. 11). Large molecules may be anchored between two beads and pulled by displacing one of the beads. This allows measurement of the bending elasticity of macromolecules as well as force-dependent macromolecular conformational changes. These types of single molecule manipulations and measurements are exquisitely sensitive and provide insight into the mechanical properties of macromolecules. In the C-Trap, a DNA molecule can be stretched, compressed, and moved throughout the flow cell in order to efficiently conduct experiments. The user has the ability to adjust the strength of the trapping, as well as change the position of the traps during the experiment[32]. Acquiring live, simultaneous data about force and DNA elongation (position of one end/bead with respect to the other) allows for valuable data collection in experiments that require DNA stretching.

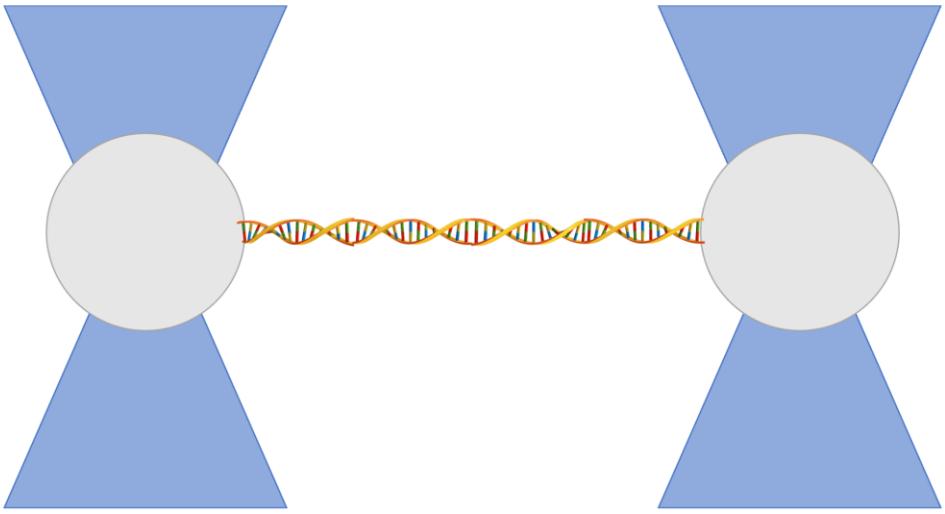

Figure 11. Schematic diagram of two optical lasers (blue), each with a single trapped bead (grey), and a tethered DNA molecule stretched in between[32].

2.4 Fluorescence and its Use in a Model System

The third and final component of the C-Trap is the internal microscopy system that allows for live visualization of fluorescent biomolecules such as appropriately labeled genetic material, proteins, beads, and other biomolecules at the single-molecule level. The confocal microscopy system in the microscope includes three lasers of wavelengths[33] 488 nm (26.7 μW), 532 nm (42.6 μW), and 638 nm (44.8 μW) that can be used either individually or in combination with each other, allowing for simultaneous visualization of multiple fluorescent signals that are excited at different wavelengths[34]. Visualization of single molecules is facilitated by the high sensitivity (single-photon counting) and speed (up to 200 lines per second)[31] of the microscope.

In addition to the traditional images and scans produced by these confocal microscopes, this system can also generate kymographs, or line-scans, while simultaneously collecting force, position, and photon data. While images and scans are useful in identifying the presence of

fluorescently-tagged molecules, the kymograph is particularly useful to reveal dynamic behavior, such as transcription elongation by RNA polymerase, because it provides a detailed graphical and time-sensitive representation of any fluorescent events, such as protein-binding or DNA breakage[31] (Fig. 12). Overall, the integration of the confocal system with the high-resolution optical tweezers consequently allows for an in-depth collection of real-time data during an experiment that can later be extensively analyzed with other computer programs.

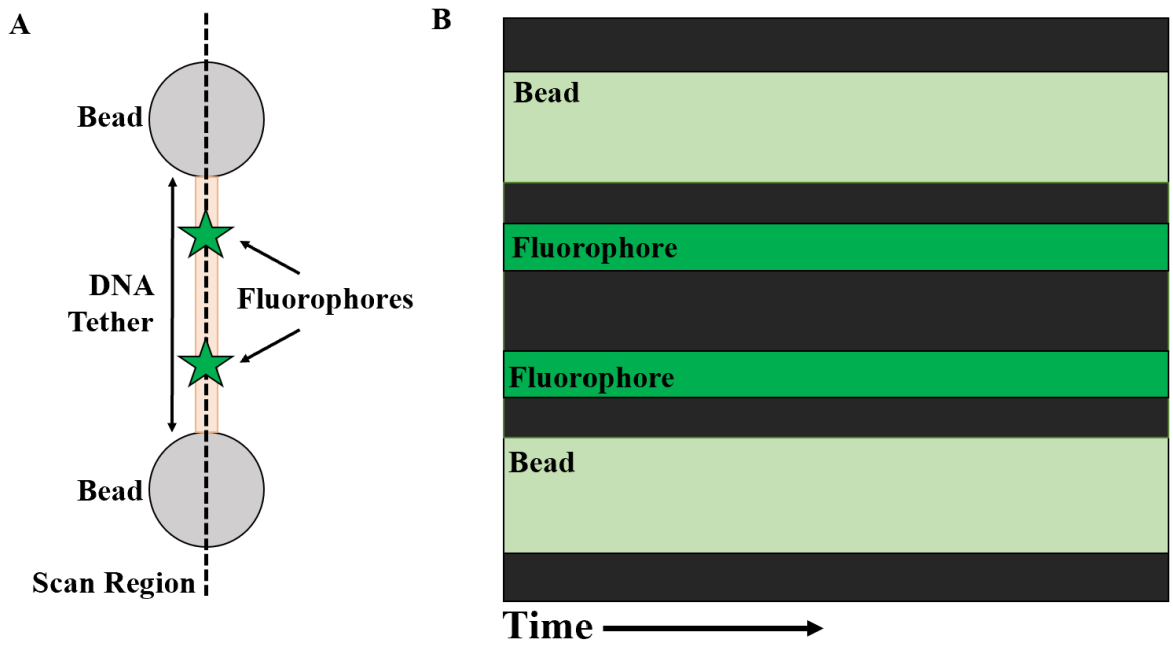

Figure 12. Schematic diagram representing the set-up for a kymograph **(A)** and the resulting kymograph **(B)**. The dotted line indicates the scanning region and the orange rectangular box represents the DNA tether.

2.5 Experimental Process and Optimization

Sample preparation for use in the C-Trap is straightforward, though it requires expertise in DNA-construct designing and preparation techniques. Typical experimental sample systems contained beads to serve as DNA handles, DNA constructs to be tethered between the beads, and any

accessory biomolecules such as enzymes, fluorescent labels, and dyes. The actual distribution of these components varies depending on the physical characteristics of the DNA construct; however, all experiments do require having DNA flowing in one channel so that it can be "fished" by the beads caught by the optical traps in another channel. As with most other biological experiments, there were many experimental conditions that required optimization before results were achieved.

The process of optimization is a long series of trial-and-error until desirable results are achieved. The preliminary conditions to be optimized included bead concentration and DNA concentration and tether-bead complex incubation time. If the bead concentration was too low, the experiment often ran overtime due to the difficulty of finding to catch in the traps; if the bead concentration was too high, uncaptured beads would knock captured beads out of the trap, thereby prolonging the bead-capturing and DNA-tethering process. Likewise, when DNA concentrations were too low, tethering was difficult to achieve. However, when the DNA concentration was too high, multiple-tether complexes prevented finding a single DNA tether. Additional parameters to optimize included pressure, which adjusted the flow rate of the samples, and trapping laser power, which determined the strength with which a bead can be held without heating the sample too much.

Beyond preliminary conditions, optimization became an important part of the fluorescent-visualization process because it determined the resolution of confocal images, as well as the strength and lifetime of the fluorescent signal. The major play-off in settings occurred with the line time (determined by scanning distance, pixel size, and pixel time) and laser intensity. When pixel time was long and laser intensity was high, the fluorescent signal was generally bright and

defined well in contrast to the background fluorescent signal; these conditions, however, can result in significant heat and energy generation, leading to DNA tether rupture, or premature extinction of the fluorescent signal. Along with these two settings, the line time was also adjusted to ensure maximum possible fluorescent signal with over-excitation of the fluorophore.

As experiments evolved, the settings often had to be readjusted to account for changes in DNA mechanical strength and fluorophore intensity. While some DNA tethers could tolerate high forces to allow intercalation of dye, other tethers were quick to break upon excitation with high intensity laser power. Similarly, while some fluorophores could generate long-lasting, strong, and defined signals with a low laser power, other fluorophores went extinct quickly after excitation or generated too broad of a signal to identify the borders well.

2.6 Advantages and Disadvantages

The C-Trap is a valuable addition to the field of biological single-molecule techniques particularly due to its combination of high-resolution dual optical tweezers, confocal microscopy, and microfluidics. While individually these techniques are popular in the field, the C-Trap's is unique in its ability to run single-molecule experiments with microscopy while simultaneously obtaining force and distance data in real-time. This method is not only user-friendly and high-performance, but it most importantly allows experimenters to collect multiple streams of data, at the same time, of a complex biological system[31].

Given the instrument's relative recent invention, however, there still remains many protocols to be developed and operating conditions to be learned. Without prior knowledge on the operations of the machine, it can be difficult to learn about the details that lie in use of the instrument. Notably, the tubing system between the syringes and flow cell is prone to clogging, especially

when used in protein- or cell-containing experiments, which makes experimental clean up and preparation lengthy and tedious.

3 Materials and Methods

3.1 DNA Tether Construction with PCR

Polymerase Chain Reaction (PCR) is a three-step cyclical reaction that aims to amplify the amount of DNA in a given sample by denaturing the dsDNA, annealing the primers to each ssDNA, and then extending the DNA with polymerase enzymes[35] (Fig. 13).

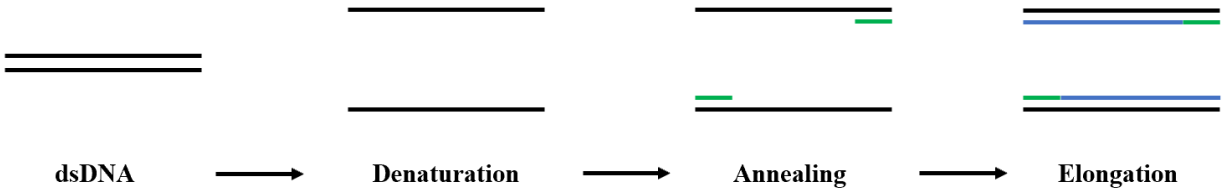

Figure 13. Schematic diagram showing the steps of PCR[35]. The template DNA strands are shown in black, primers shown in green, and elongated replicated strands in blue.

Using PCR, a DNA amplicon of length 13.791 kbp (abbreviated to 14 kbp) was constructed using a biotin-labeled forward primer (GGAGCCTGTGTAGC) and digoxygenin-labeled reverse primer (CATCGCAACCGCATC) with the pDM_S1A_400_sq plasmid of length 13.992 kbp (Fig. 14) and then purified using the GeneJet PCR Cleanup Kit (Thermo Scientific, Waltham, MA). Because both of the primers were labeled with either biotin or digoxygenin, each end of the DNA tether was labeled with a single biotin or digoxygenin.

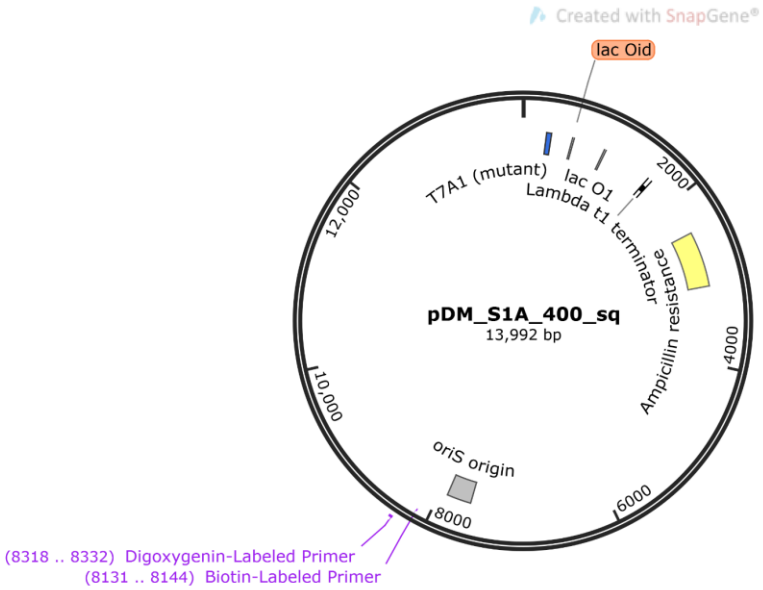

Figure 14. Plasmid map showing the two primers and plasmid used to construct the 14 kbp tether[36].

3.2 DNA Tether Construction with Labeled Nucleotides

PCR was additionally used to generate a DNA construct of length 11.962 kbp (abbreviated to 12 kbp) using the fluorescently labeled cytosine nucleotide, Cy5-dCTP. The reaction was run using the pDM_S2_400_sq plasmid of length 13.985 kbp (Fig. 15), a biotin-labeled forward primer (GGAGCCTGTGTAGC), a digoxigenin-labeled reverse primer (TGCTAGGTTAGCATTAAGA), and a ratio of 1:4000 Cy5-dCTP, after which the final DNA fragment was purified using the GeneJet PCR Cleanup Kit (Thermo Scientific, Waltham, MA).

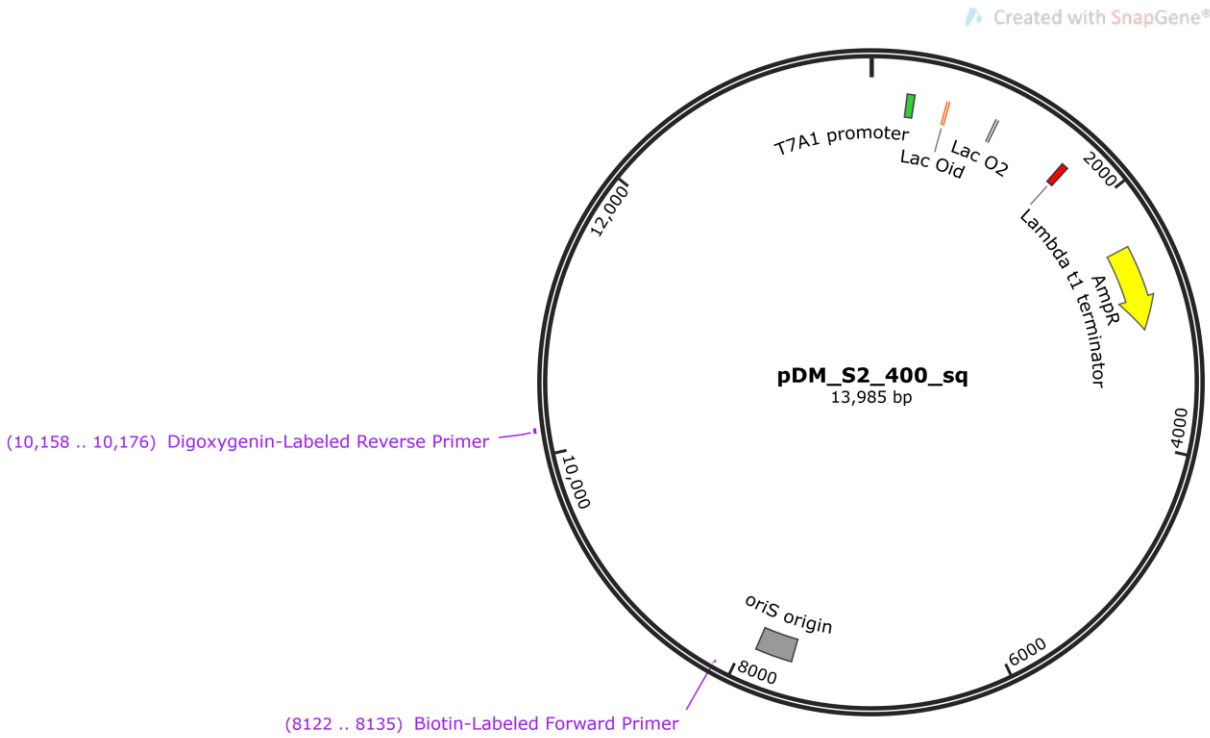

Figure 15. Plasmid map illustrating the two primers and plasmid used to construct the 12 kbp tether for Cy experiments[36]. Binding regions of RNAP are found at the T7A1 promoter and AmpR gene.

The final construct also contained a biotin label on one end and a digoxygenin label on the other end. Based on the ratio of labeled nucleotides used and the length of the final tether, it is expected that each DNA construct includes 1-3 Cy5 fluorophores. An additional DNA construct was created using the same protocol, except for the replacement of Cy5-labeled dCTP (Cy5-dCTP) with biotin-labeled dTTP (bio-dTTP), to serve as a positive control. For RNAP experiments, the final tether was made from the same plasmid and primers and without Cy5-dCTP to generate an unlabeled tether with RNAP binding regions at the T7A1 promoter and Ampicillin Resistance Gene (AmpR).

3.3 DNA Tether Purification and Characterization with Gel Electrophoresis and AFM

To verify that all PCR constructs had the proper length, gel electrophoresis assays run in 1% agarose gel, TAE buffer, and ethidium bromide; all DNA samples were loaded with DNA loading dye and compared to the Quick-Load 1 kb Plus DNA Ladder (New England Biolabs, Ipswich, MA). The concentration of all amplicons was obtained using a Nanodrop Spectrophotometer, which returned the DNA concentration in ng/µL. Additionally, the bio-dTTP construct was analyzed with atomic force microscopy (AFM) to confirm the presence of substituted nucleotides in the DNA construct to ensure the polymerase enzyme used in the PCR properly incorporated the labeled bases (Fig. 16).

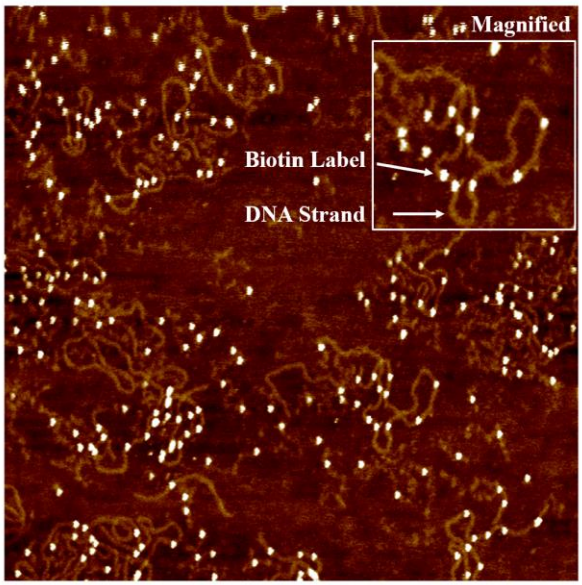

Figure 16. AFM image confirming the incorporation of biotin-labeled dTTP in the DNA construct. The DNA strand is the orange, curled line. The biotin label is the white circle.

3.4 Sample and Flow Cell Preparation for C-Trap Use

All solutions were prepared on the work bench and then transferred to the syringes that connect to the flow cell with tubing (Fig. 17). The general solvent in all channels for non-transcription experiments was phosphate buffer solution (PBS, 2 mM EDTA, 2 mM Sodium Azide). In these experiments, Channel 1 was prepared by diluting polystyrene streptavidin beads of 2.07 um diameter (Spherotech, SVP-20-5) in PBS; first, 2 µL of beads were diluted and mixed thoroughly with 8 µL of buffer, and then 1.25 µL of the dilution mixture was further diluted with 500 µL buffer. Channel 2 consisted of buffer. To prepare Channel 3, 1 µL DNA constructs (2nM) were incubated in the dark at room temperature with 2 µL anti-digoxigenin-coated polystyrene beads of 2.07 um diameter (Spherotech, DIGP-20-2) and 2 µL buffer. After incubation, the mixture was further diluted in 500 µL buffer and loaded into the syringe. For experiments using the 14 kbp tether, Channel 4 was loaded with SYBR green DNA-intercalating dye (Invitrogen, S7563) diluted in buffer; 0.2 µL of dye was mixed thoroughly with 1 mL buffer.

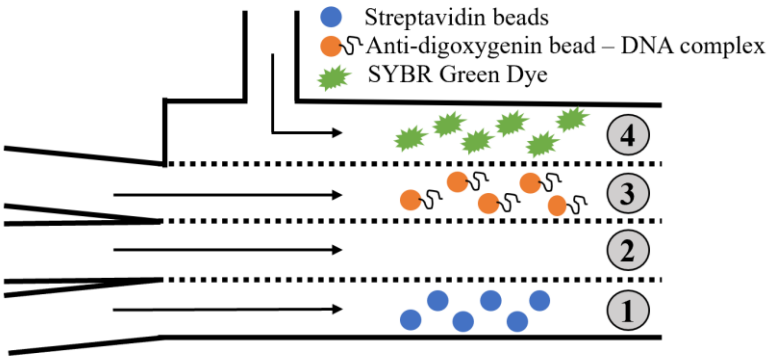

Figure 17. Schematic diagram representing the flow cell channel contents for non-RNAP experiments. Channel 1 contains streptavidin beads, Channel 2 contains buffer, Channel 3 contains anti-digoxygenin bead – DNA complexes, and Channel 4 contains SYBR green DNA-intercalating dye.

For experiments conducted with RNAP, the flow cell configuration varied from the visualization experiments (Fig. 18). Prior to loading the channels, biotin-labeled RNAP (125 nM) was incubated with Cy3-labeled streptavidin protein (25 μM) for 30 minutes without light at room temperature. In a separate tube, 1 μL of unlabeled 12 kbp construct (2 nM) was incubated with 1.25 μL of diluted streptavidin beads (2 μL stock of beads in 8 μL buffer) for 10 minutes at room temperature. These two incubations were then combined and incubated again for 30 minutes without light at room temperature, then diluted with 500 μL buffer and loaded in Channel 1. Channel 2 consisted of buffer, Channel 3 contained 2 μL anti-digoxygenin beads diluted in 500 μL buffer, and Channel 4 contained diluted nucleoside triphosphates (NTPs). The main solvent in all these channels was transcription buffer (20 mM Tris-Glutamate at pH 8.0, 50 mM Potassium-Glutamate, 10 mM Magnesium-Glutamate, 1 mM dithiothreitol).

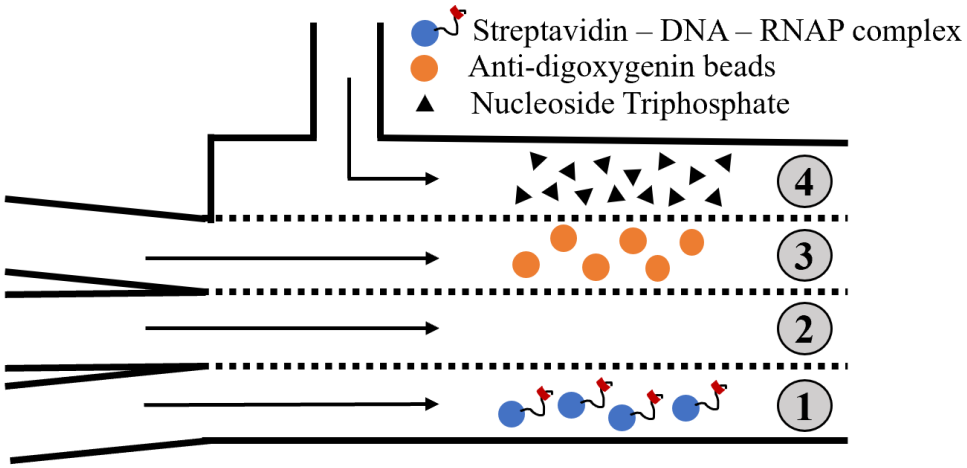

Figure 18. Schematic diagram representing the flow cell channel contents for RNAP experiments. Channel 1 contains streptavidin – DNA – RNAP complexes, Channel 2 contains buffer, Channel 3 contains anti-digoxygenin beads, and Channel 4 contains NTPs.

Once all required channels were loaded with their contents, the exterior of the flow cell was prepared. One drop of water was placed on the lower objective, and then the objective was lifted until the water made contact with the bottom surface of the flow cell. Next, two drops of oil were added to the top surface of the flow cell. The lower objective was then focused using the z-axis diagnostic camera on BlueLake, and then the condenser was lowered until a good moon was observed on the user interface (Fig. 19). A good moon must be perfectly round and should contain 6 to 7 dark horizontal stripes.

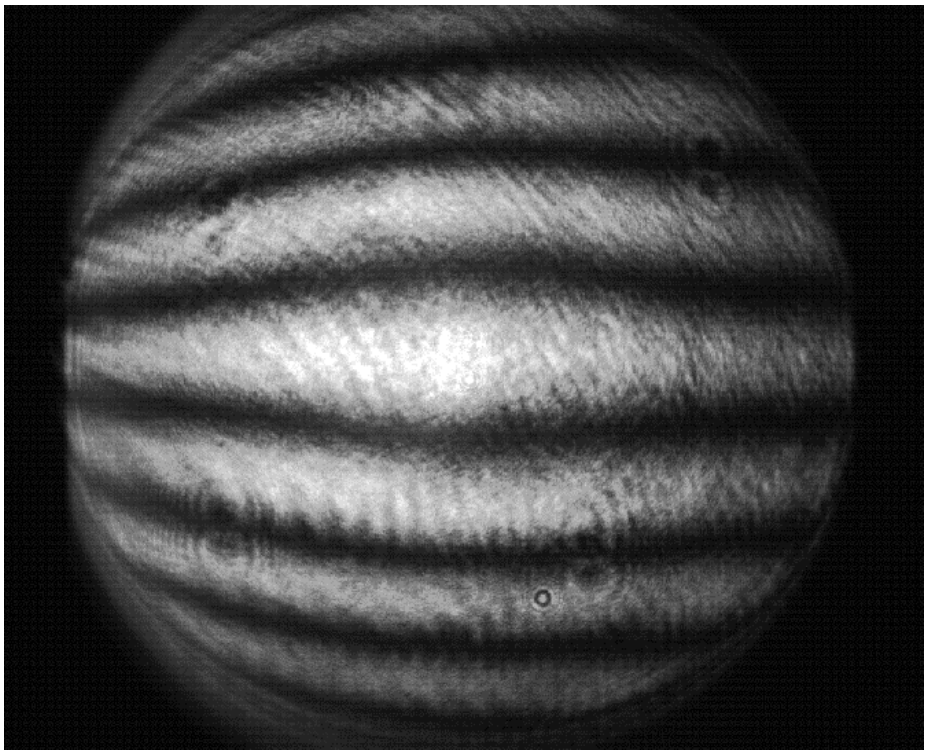

Figure 19. A good moon, indicating adequate focus of the lower objective and condenser.

3.5 Tether Capturing and Manipulation in the C-Trap

In general, tether capturing in the C-Trap required that labeled DNA tether be bound to an anti-digoxygenin bead on one end and a streptavidin bead on the other end. Because tethers were

complexed to one bead prior to loading in the syringes, the only bond that needed to be formed in the flow cell was the un-incubated bead to the matching labeled end of the DNA (Fig. 20). It was important to have the DNA-bead complex in Trap 1, on the left, to ensure the downstream flow would extend the DNA tether to reach the bead in Trap 2.

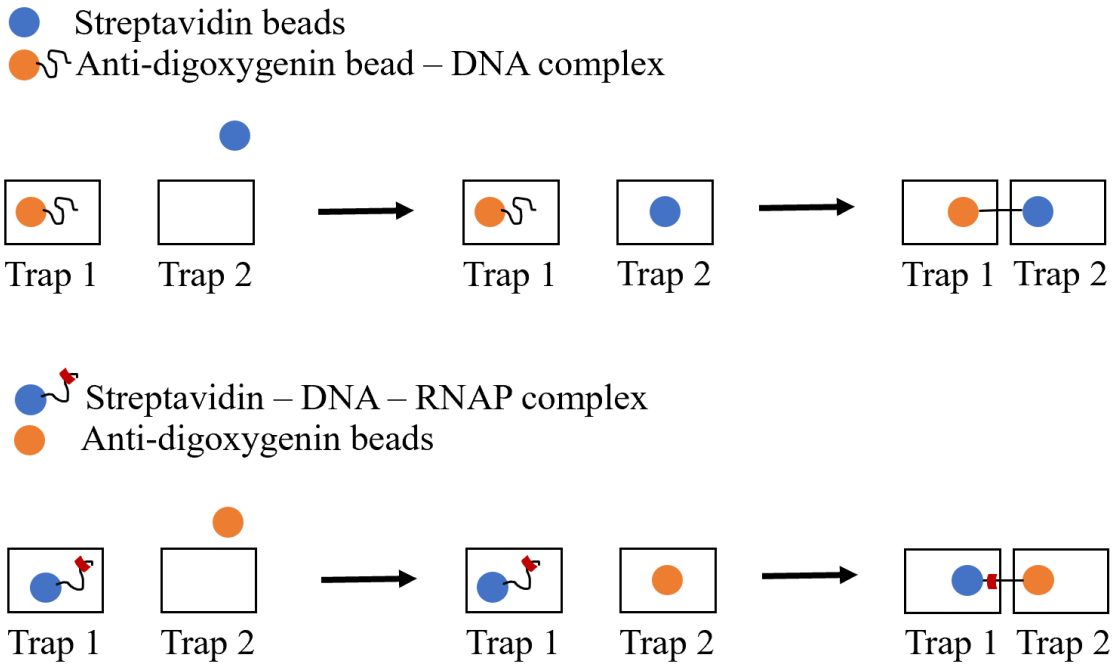

Figure 20. Schematic diagram representing the stepwise process of capturing tethers for non-RNAP (top) and RNAP (bottom) experiments. A bead in the box indicates that it has been trapped by the optical tweezer trapping laser.

For the 14 kb tether, the tether capturing protocol involved capturing a streptavidin in one trap in Channel 1, capturing a digoxygenin bead in the second trap in Channel 3, and finally reorienting the beads in Channel 2 so that the anti-digoxygenin bead was directly upstream of the streptavidin bead. Once the beads were in the region of interest and recognized by the C-Trap, they were horizontally moved to be approximately 1.00 – 2.00 μm apart. After waiting a few

seconds, the beads were horizontally moved apart until an increase in force was detected. The force-extension curve of the live data was compared to the system's model curve generated based on the worm-like chain model[11,12].

For the 12 kbp construct, after a tether was detected by an increase in force, the beads were reoriented to have the anti-digoxygenin bead directly downstream from the streptavidin bead (Fig. 21). Once the beads were repositioned, they were once again moved apart to stretch the tether.

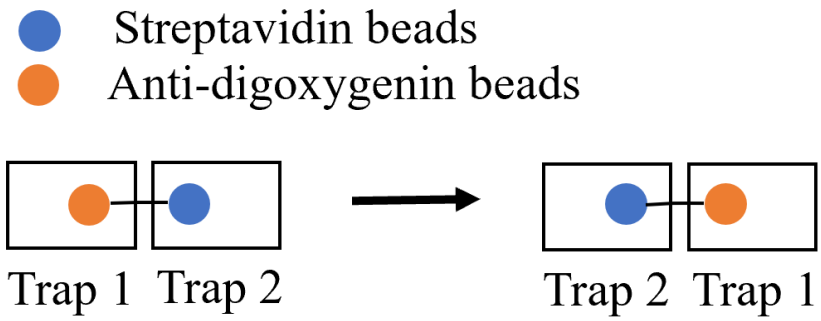

Figure 21. Reorientation of beads to ensure anti-digoxygenin bead is downstream.

In the case that multiple tethers were found in either experiment, the beads were slowly moved apart to break additional tethers until only one remained. In the case that no tethers were found after three rounds of approaching and separation cycles, the beads were discarded and replaced with new beads.

3.6 Confocal Microscopy with the C-Trap

The C-Trap performs confocal line scans of a DNA tether between two beads, which can be viewed in temporal sequence (kymographs). All kymographs were generated at room

temperature and in the presence of flow. Kymographs of the 14 kbp tether were generated by exciting intercalated SYBR green dye with the 488 nm laser at various laser intensities. The line scan was set to range between the inner surface of both beads (Fig. 22). For the 12 kbp DNA tether containing Cy5-labeled bases, kymographs were generated in Channel 2. The fluorophores were excited with the 638 nm laser at various intensities.

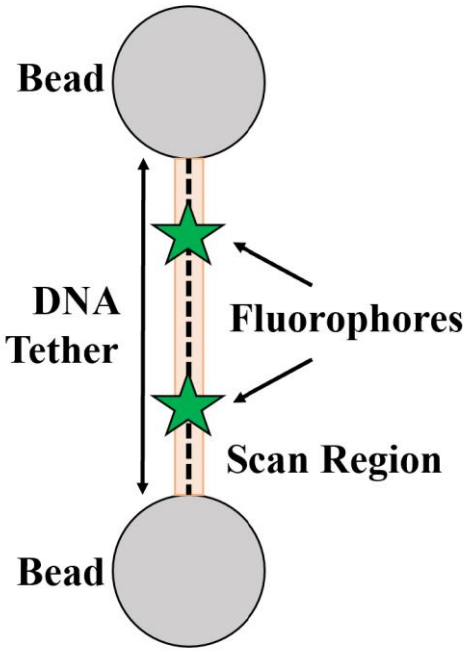

Figure 22. Schematic diagram illustrating the modified line-scan dimensions to minimize autofluorescence of beads. The scan region is indicated by the dotted line and the DNA tether is represented by the orange rectangle.

3.7 Oxygen Scavenger Methods for Improved Fluorescent Imaging

Oxygen scavenging methods were implemented to increase the lifetime and decrease the background of the fluorescent signals of interest. Because oxygen reacts with the fluorescent materials in the samples, oxygen scavenger systems are able to decrease unwanted fluorescent signals in solution. While multiple methods were tested, the most successful procedure used a

glucose oxygen scavenger system (50 mM Glucose, 7.5 units/mL glucose oxidase, 1000 units/mL catalase) and Trolox (100 mM) in Channel 2 and Channel 4.

Other attempted methods included degassing the PBS buffer to significantly reduce the number of gas particles in solution, though there was no significant difference in fluorescent lifetime with this method. To create a barrier between the aqueous layer and the air, a layer of mineral oil was placed on top of the degassed buffer in the syringe, however this method did not significantly improve confocal images either.

4 Results and Analysis

4.1 Force-Extension Curves Prove DNA Tethering

Using the high resolution dual optical tweezers in the C-Trap machine, force-extension curves were obtained to identify single DNA tethers. Based on the rupture force and the maximum length, force-distance curves could indicate whether single tethering, multiple tethering, or no tethering was obtained. Preliminary experiments were conducted with a DNA tether of length 14 kbp. After inputting the tether length into the C-Trap software, a theoretical curve for a single tether is produced based on the worm-like model and serves as a reference during the experiment[12]. For a tether of this length, the reference curve begins to increase in force near 4.25 μm.

The experiments showed that nearly all beads contained multiple tethers, indicating that the tether handles have a high affinity for the DNA. In a force-extension curve, multiple tethering was indicated by a premature increase in force. If multiple tethers were presenting, the beads were gradually separated to increase tension and induce ruptures until only one tether remained

intact. The rupture of the tether coincides with a sudden decrease in force; in multiple tethering, these drops occur frequently as the beads are pulled apart (Fig. 23).

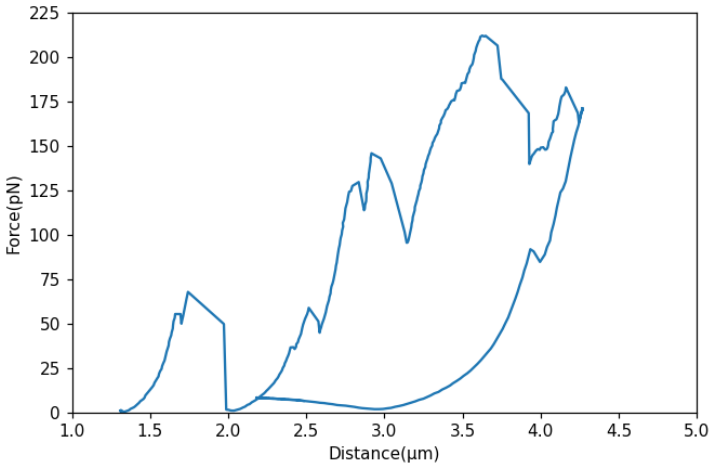

Figure 23. Force-distance curve of multiple 14 kbp-long DNA tethers[37].

Our experiments with this DNA sample showed that the number of tethers connecting the two beads in the dual optical tweezers system could efficiently be reduced to a single tether that closely follows the reference curve generated by the worm-like chain model[12] (Fig. 24).

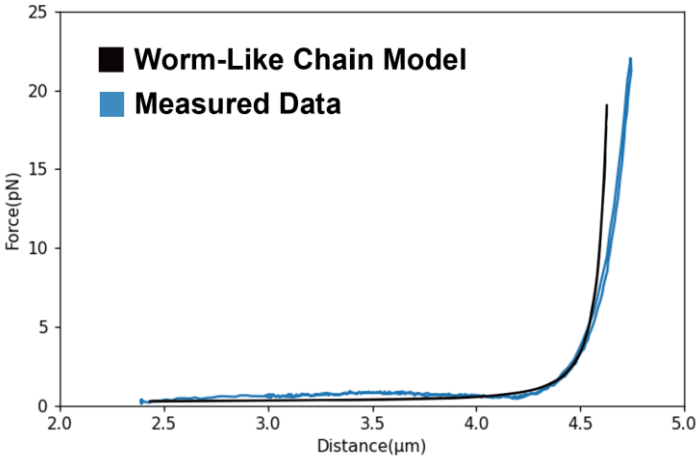

Figure 24. Force-extension curve of a single 14 kbp-long tether superimposed with the reference curve[12,37].

4.2 Confocal Imaging with Fluorescent Intercalator Verifies DNA Tethering

After confirming the protocol to assemble DNA tether with force-extension curves, entire DNA tethers were visualized using the confocal microscope and SYBR Green, an intercalating dye. Real-time force data was used to confirm the presence of a tether while taking continuous kymographs (see Materials and Methods and Fig. 25). Brief fluorescent signals were observed with the 14 kbp-long DNA sample at various laser powers, forces, and bead distances.

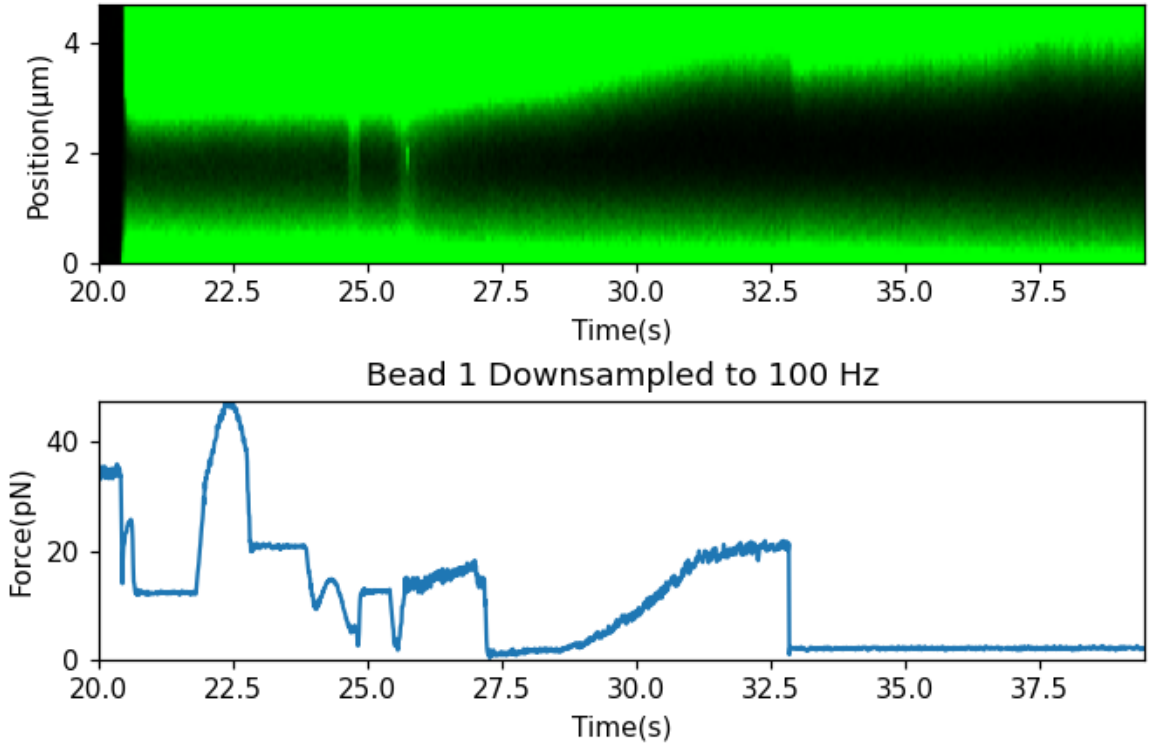

Figure 25. Kymograph and force-time curve of the 14 kbp-long DNA sample taken with the 488 nm laser at 7.5% power[37].

All trials revealed that the force experienced by the tether needed to be relatively high to facilitate intercalation of the dye, approximately 45 pN, but that the confocal laser power did not need to be high; tethers were observed with as little as 2% intensity. This force of 45 pN is

expected and similar to other studies reporting a 45 pN force to visualize a signal[32]. All trials also revealed that there is a substantial amount of background fluorescence coming from the beads, which was later reduced using an oxygen scavenger and bovine serum albumin (1%) in the buffer. Because such a high force is needed for the fluorescent dye to become intercalated in the tether and thus illuminate the tether, the majority of DNA tethers did not show long-lasting signals due to premature rupture upon extension. It was possible, however, to recover fluorescence by briefly increasing the force again to allow re-intercalation of the dye (Fig. 26). The increased force jumps below are due to the movement between Channels 2 and 4, not the extension of the tether. It is possible that these force jumps contributed to intercalation and signal visualization, or that moving between channels caused the slacked tethers to enter the focal plane.

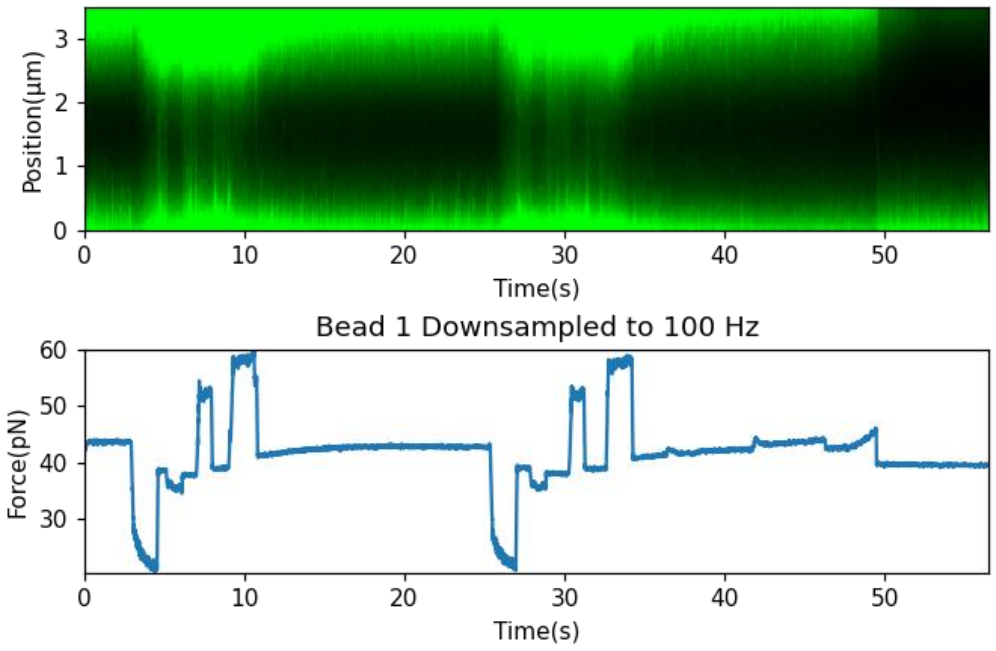

Figure 26. Kymograph and force-time curve of the 14 kbp DNA sample taken with the 488 nm laser at 2.5% power[37].

4.3 Confocal Imaging of Fluorescently-Labeled DNA Verifies DNA Tethering

As an alternative to the intercalator dye, which required the application of high forces that compromised the tether integrity, we imaged DNA tethers sparsely labeled with Cy5, a red fluorescent dye. In contrast to visualizing the entire DNA strand, we were attempting to detect single Cy5 molecules along the DNA (Fig. 27). Preliminary results indicated that it is possible to see a Cy5 signal between the two beads, but the signal lasted only 5 to 25 seconds before diminishing and, eventually, disappearing. Because a single dye molecule would suddenly disappear instead of diminishing, this result is indicative of either multiple Cy5 signals in this region or an out-of-focus scanning region[38].

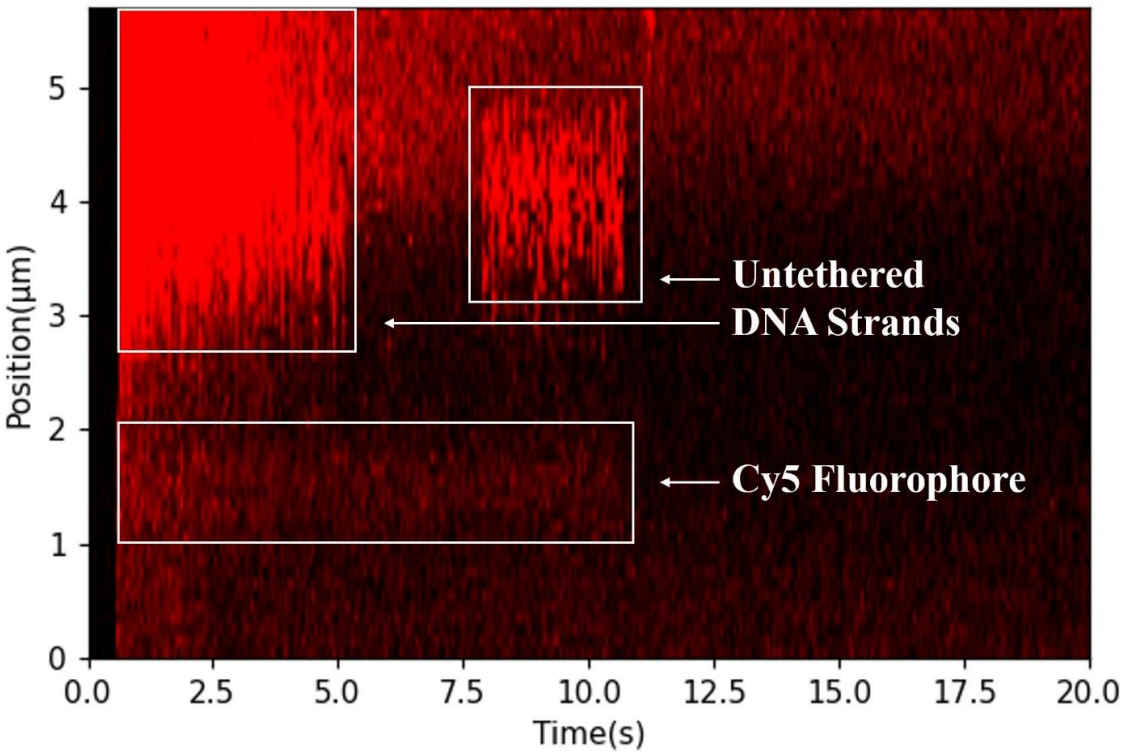

Figure 27. Annotated kymograph of fluorescence from a 12 kbp Cy5-substituted DNA tether taken with the 532 nm laser at 100% power[37].

Preliminary results showed that DNA strands emanating from the streptavidin-coated bead contributed background fluorescence, so the flow rate was increased and the orientation of the beads was reversed in an attempt to obtain a clearer image (Fig. 27). This produced a lower background and somewhat stronger signal (Fig. 28). However, the fluorescence between the beads was not as punctate as what has been published in the literature by others imaging single dyes[38].

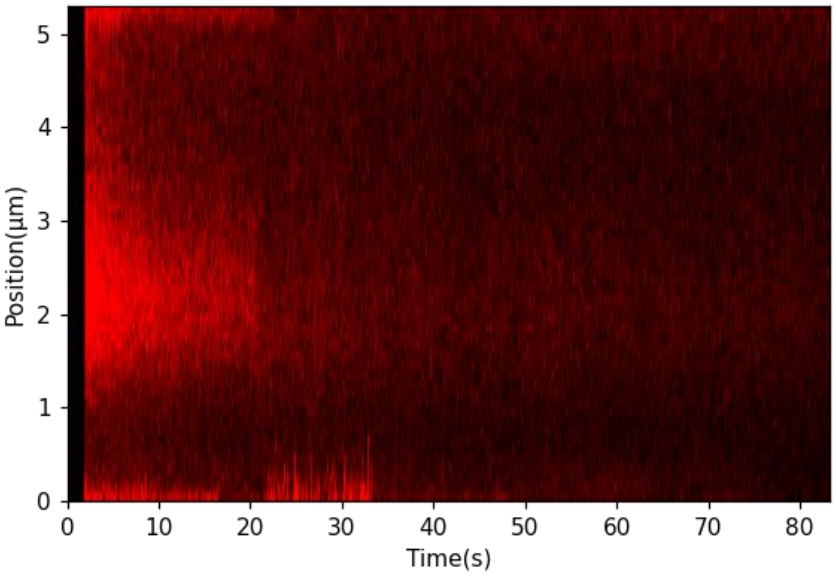

Figure 28. Kymograph of a DNA tether substituted with a multiple Cy5[37]. Taken with the 532 nm laser at 50% power.

A single fluorophore will be convolved by a point spread function of the imaging lens, so, the image pixel intensity was compared with a Gaussian curve to estimate the width of the observed spot using ImageJ[39]. Results showed that this kymograph of a single fluorophore fits a normal probability distribution but it diminished gradually instead of suddenly and was wider than half of the wavelength of the 650-750 nm light emitted (Fig. 29). A histogram was also plotted on the

X-axis using Image J and showed the intensity of the fluorophore decreases exponentially as a function of time, indicating there must be multiple fluorophores in this region[39] (Fig. 29).

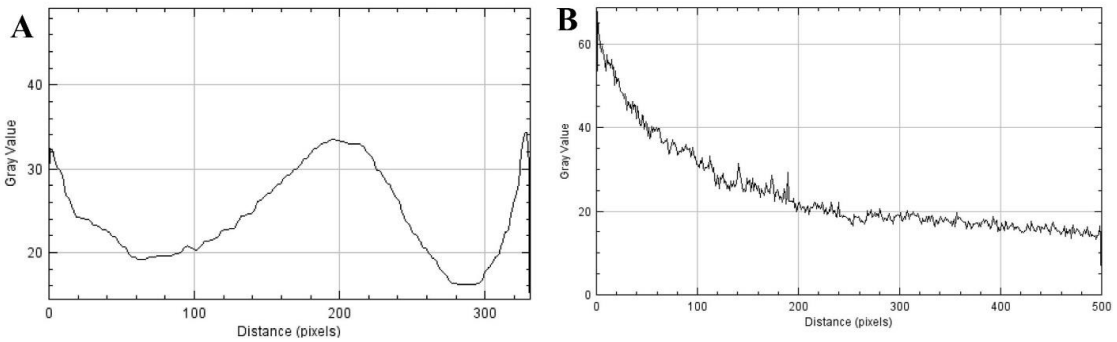

Figure 29. Profile analysis of the previous kymograph[39] (Fig. 28). **(A)** Gaussian Distribution with a peak at 200 pixels representing the single Cy5 fluorophore. **(B)** Decay of fluorescent signal as time progresses.

The sensitivity of the Cy5 signal and lifetime of the fluorescent emission was greatly improved when the focus of the instrument was adjusted. While the beads in all experiments were in focus as indicated by the software's ability to recognize the beads, in order to focus the confocal microscope on the fluorescent signal emanating from the DNA tether, it was necessary to move the beads out of focus in order to provide clearer, stronger, and longer-lasting signals (Fig. 30).

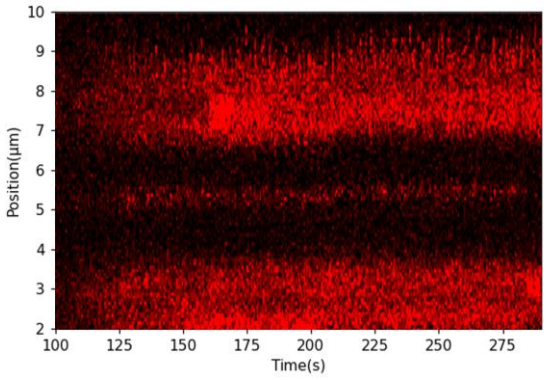

Figure 30. Kymograph of a DNA tether labeled with a single Cy5 fluorophore[37]. Taken with the 532 nm laser at 50% laser power.

4.4 Confocal Microscopy Confirms RNAP Binding to DNA

In addition to visualizing single fluorophores along a DNA tether, the binding of Cy3-labeled RNA polymerase to an unlabeled 12 kbp tether was visualized with fluorescence. The Cy3 label on the protein was illuminated with the 532 nm laser with an operating power of 10%. The construct had two expected sites of RNAP binding, the T7A1 promoter and the AmpR promoter (Fig. 31B); RNAP generally bound to either one or both of these sites during experiments. As the tether was stretched slightly, bound RNAP held the same position that displaced accordingly (Fig. 31A).

In addition to RNAP binding, kymographs showed translocation behaviors on the DNA strand (Fig. 31C). After visualization of RNAP binding to DNA, the complex was moved to a buffer channel containing NTPs in order to observe transcription. Although we are still not able to see RNA transcribe the DNA, the clear and strong signal produced by Cy3 on RNAP provides confirmation that RNAP movement will be visible once we can facilitate transcription.

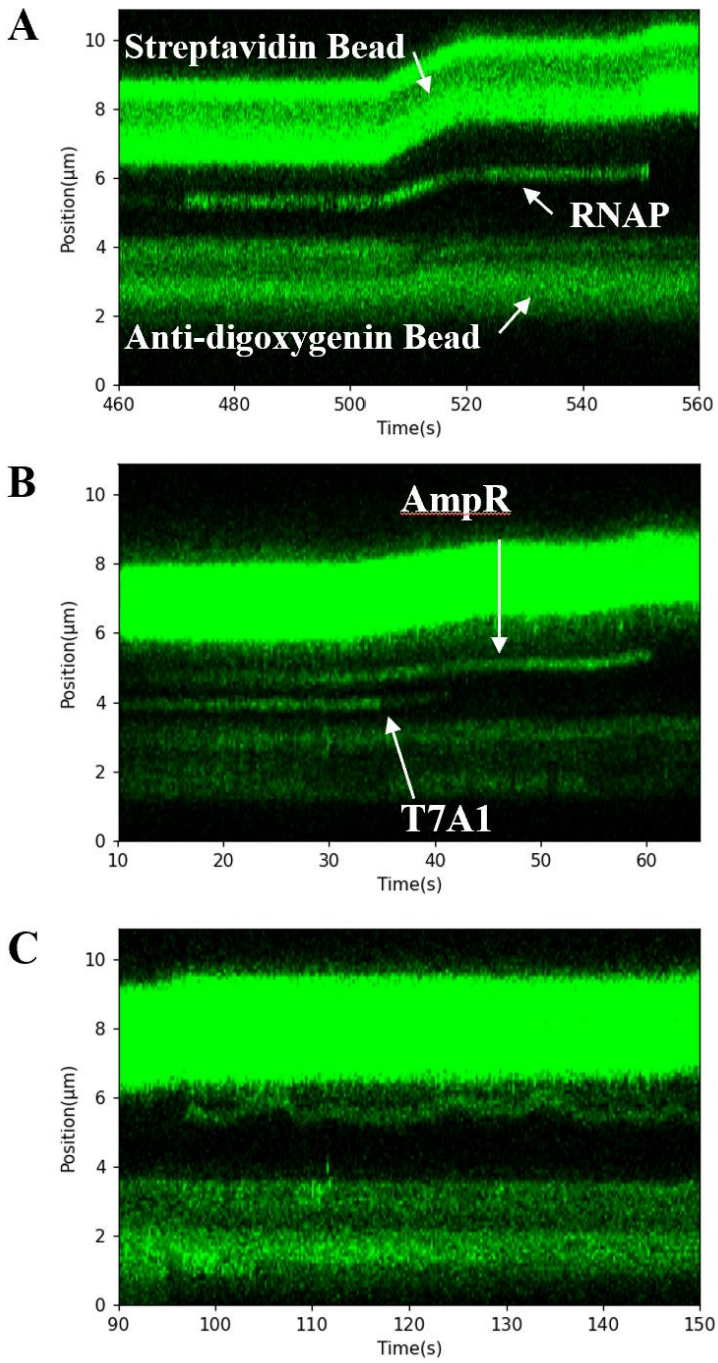

Figure 31. Kymographs show RNAP bound at one **(A)** or two **(B)** sites, and another one with an enzyme randomly diffusing in the 5-6 μm range **(C)** on the unlabeled 12 kbp DNA tether[37]. All kymographs were taken with the 532 nm laser at 10% power. Beads and RNAP are labeled in **(A)**.

4.5 Manipulation of Confocal Images for Optimized Fluorescent Visualization

While the C-Trap user interface softwares, BlueLake and LakeView, function to display force-extension curves and confocal images, further analysis must be conducted in Python in order to isolate and highlight data of interest. There is a published Python script that generates a graphical user interface (GUI) that allows users to display force-extension curves, force-time curves, and kymographs in a publishable format (Fig. 32). While there are other functions such as data export, the plotting functions were extensively used in the analysis of force-extension curves and kymographs.

Upon uploading, force-extension curves are generated using the “Draw Plot” function. The displayed force can be broken down into X and Y forces, or the sum of both, from either Trap 1 or Trap 2. Force-extension curves for this project were displayed using X and Y sum of Trap 1 forces, and the scale of the graph was adjusted using the “Axis Options” table. The final graph is then exported as a PNG.

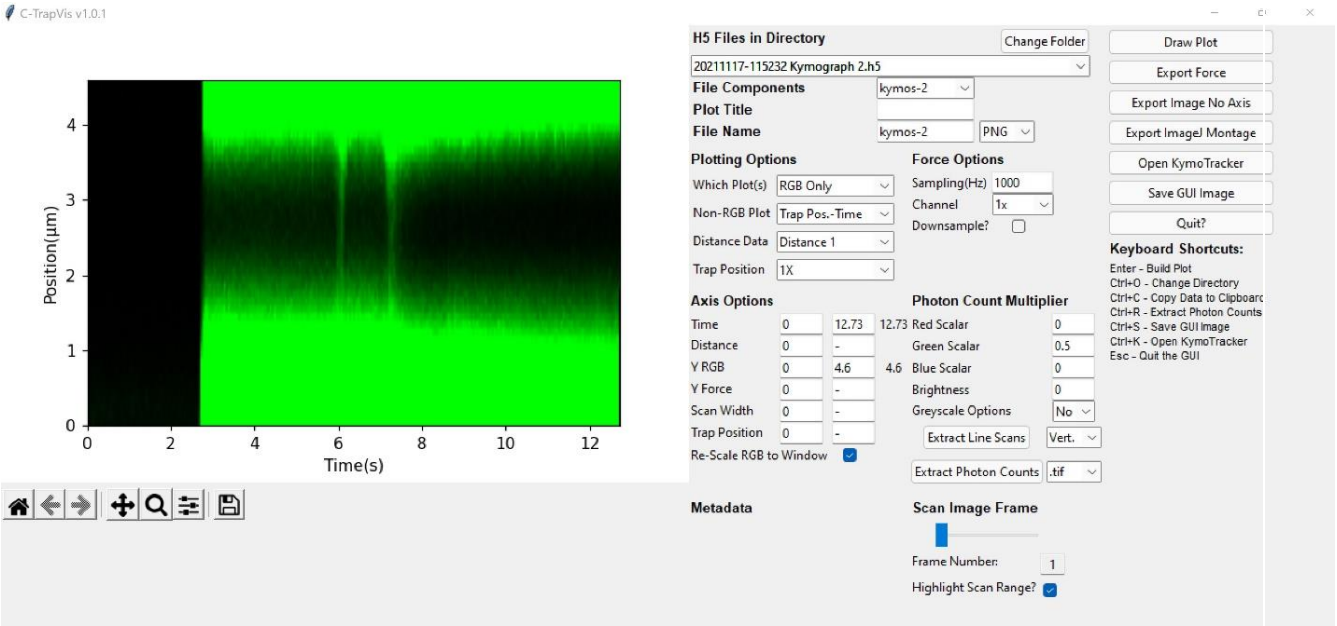

Figure 32. Screenshot of the Python GUI used to generate force-extension curves, force-time curves, and kymographs[37].

In addition to force-extension curves, kymographs can be uploaded and filtered to maximize the fluorescent signal resolution and minimize the background fluorescence or auto-fluorescent of the beads (Fig. 33). Upon uploading the kymograph, the intensity of red, blue, and green emission signals can be adjusted using the “Photon Count Multiplier” table; when there is only one emission color, colors not emitted were set to zero. The kymographs can also be cropped on both the X and Y axis using the “Axis Options” table to zoom in on the signal of interest. It is also possible to plot a force-time curve under the kymograph using the “Which Plot” button to visualize what the force looked like at each moment of time in the kymograph (Fig. 25). Overall, this GUI has allowed for production of optimal kymographs, force-extension curves, and force-time curves.

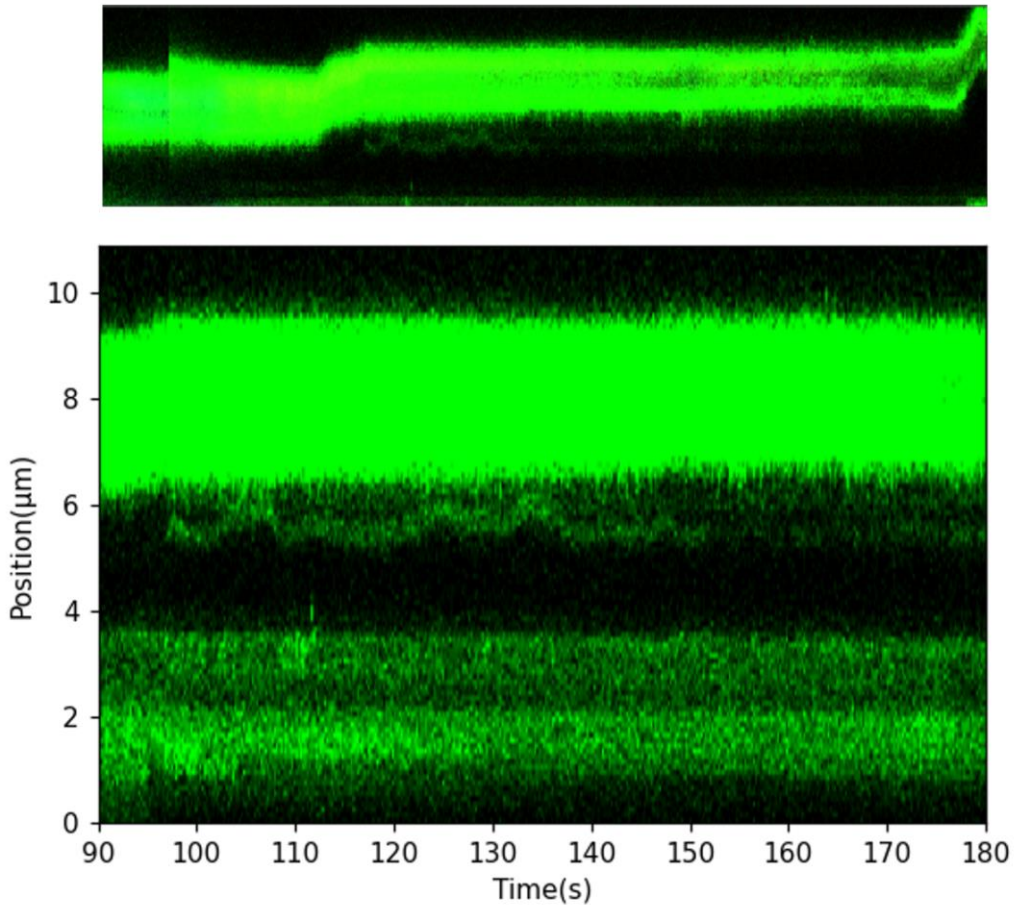

Figure 33. Kymographs before (top) and after (bottom) analysis with the Python GUI[37].

4.6 Troubleshooting

Issues experienced when conducting experiments with the C-Trap included mechanical problems, like improper laminar flow, and problems relating to the chemical environment. Problems with the laminar flow of the cell were easily detected by observing either unequal volume displacement in syringes over time or by observing the flow paths of the cell, such as a channel with flow wider than expected. Although the liquids were clear, it was possible to determine the borders of flow by determining where the beads were flowing. These mechanical problems were generally caused by clogging in the flow cell and were resolved by flushing the

syringes, tubing, and cell at 1.7 bar by following the Lumicks u-Flux Flow Cell Cleaning Protocol[40].

Issues with the chemical environment were more difficult to resolve and required more extensive experimental trials to resolve. While the confocal microscope was easy to operate, it was difficult to discover a chemical environment and microscope settings with which to visualize DNA. Several things increased the background fluorescence in the field of view, which made it more challenging to see the fluorescent signal coming from the DNA. First, the polystyrene anti-digoxygenin and streptavidin beads had very high levels of fluorescence. These beads can be substituted with either silicon beads or polystyrene beads with a smaller diameter and less surface area upon which fluorescent material can accumulate. However, the smaller beads compromised the efficiency of tether capture.

Second, when using an intercalating dye, the tether had to be stretched to a high force to favor intercalation and visualize the SYBR Green dye. Often, the tethers quickly ruptured when held at high tension. Third, in the experiments with the Cy5-labeled DNA tether or the Cy3-labeled RNAP, the single molecule fluorescent signal was short-lived and larger in size than expected. When an adequate oxygen scavenging system was included in the buffer, the settings of the kymograph (line scan rate, pixel size, pixel time) could finally be optimized to maximize the intensity and resolution of the fluorescent signal. This issue was resolved after trial-and-error experiments adjusting the flow rate of the solution and the focus of the microscope, which revealed that stopped-flow conditions and seemingly out-of-focus beads in the optical trap resulted in the clearest signal from Cy fluorophores. Although stopped-flow conditions minimized the movement of DNA and made single fluorescent signals clearer, the background

fluorescence often became too high without a constant flow newly replenished oxygen scavenger and consequently all kymographs were taken in the presence of a slow flow.

5 Discussion and Conclusion

5.1 C-Trap Allows for Visualization of a Single DNA Tether and RNAP

The high resolution dual optical tweezers of the C-Trap are a useful tool for manipulating and detecting DNA tethers because the trapped DNA molecule can be moved between buffers in different channels. Real-time force, position, and fluorescent signal data can be measured throughout the experiment, which allows for correlation of information about the extension and tension in the DNA, with the location of DNA-binding proteins along the DNA tether. Visualization of the position of fluorescently-labeled RNA polymerase on 12 kbp DNA tethers indicates that this instrument can be used to track transcriptional elongation.

5.2 Optimization of Confocal Settings Improves Visualization of Fluorescent Signals

Previously published studies established that it was possible to use confocal microscopy to visualize DNA, however experimental protocols with the C-Trap's confocal microscope were fairly limited and required extensive experimentation to generate satisfactory images. For both experiments, with the DNA-intercalating dye and the fluorescently-labeled nucleotides, the chemical environment and confocal settings were manipulated substantially to create images with long-lasting and high-contrast fluorescent signals. This work ultimately provides framework for future transcriptional experiments and assays in which the fluorescent signal must be long-lived for continuous detection throughout transcriptional assays and experiments.

6 References

1 Francis S. Collins, "Double Helix", (National Human Genome Research Institute), Vol. 2022.

2 Jack Y. Ghannam; Jason Wang; Arif Jan, "Biochemistry, DNA Structure", in *StatPearls [Internet]* (StatPearls Publishing, 2021).

3 User:G3pro at en.wikipedia.org, "Phosphodiester bonds (PO_4^-) between nucleotides. Which presents Thymine (T) and two molecules of Adenine (A).", edited by PhosphodiesterBondDiagram.png (Wikipedia, 2010).

4 "DNA-structure-and-bases", edited by DNA-structure-and-bases.png (Wikipedia, 2006), Vol. 36 KB.

5 Henderson James Cleaves II, "Watson-Crick Pairing", in *Encyclopedia of Astrobiology* (Spring, Berlin, Heidelberg, 2011).

6 MIT, "The normal, hydrogen-bonded base pairs found in DNA", (Ars Technica, 2014).

7 M. Polo Camacho, "Beyond descriptive accuracy: The central dogma of molecular biology in scientific practice," Studies in History and Philosophy of Science **86**, 20-26 (2021).

8 Vicente Tordera View ORCID ProfileJosé E. Pérez-Ortín, Sebastián Chávez, "Homeostasis in the Central Dogma of Molecular Biology: the importance of mRNA instability," bioRxiv (2019).

9 John F. Marko, "1 - DNA Mechanics," Nuclear Architecture and Dynamics **2**, 3-40 (2018).

10 Iddo Heller; Tjalle P. Hoekstra; Graeme A. King; Erwin J. G. Peterman; Gijs J. L. Wuite, "Optical Tweezers Analysis of DNA-Protein Complexes," Chemical Reviews **114** (6), 3087-3119 (2014).

11 Xiaolan Li; Charles M. Schroeder; Kevin D. Dorfam, "Modeling the stretching of wormlike chains in the presence of excluded volume," Soft Matter **11**, 5947-5954 (2015).

12 C. Bouchiat; M.D. Wang; J.-F. Allemand; T. Strick; S.M. Block; V. Croquette, "Estimating the Persistence Length of a Worm-Like Chain Molecule from Force-Extension Measurements," Biophysical Journal **76** (1), 409-412 (1999).

13 Meng-Lun Hsieh; Judith Borger, "Biochemistry, RNA Polymerase", (StatPearls Publishing, Treasure Island, FL, 2021).

14 "9.2: Transcription", (2021).

15 Yikrazuul, "base pair Adenine Uracil (AU)", edited by Base pair AU.svg (Wikipedia, 2013), Vol. 25 KB.

16 Anthony A. Mercadante; Manjari Dimri; Shamim S. Mohiuddin, "Biochemistry, Replication and Transcription", (StatPears Publishing, Treasure Island, FL, 2021).

17 Vitaly Epshtein; Francine Toulm; A.Rachid Rahmouni; Sergei Borukhov; Evgeny Nudler, "Transcription through the roadblocks: the role of RNA polymerase cooperation," The EMBO Journal **22** (18), 4719-4727 (2003).

18 Ping Xie, "Model of the pathway of -1 frameshifting: Long pausing," Biochemistry and Biophysics Reports **5**, 408-424 (2016).

19 Wen-Qiang Wu; Xiahong Zhu; Chun-Peng Song, "Single-molecule technique: a revolutionary approach to exploring fundamental questions in plant science," New Phytologist **223** (2), 508-510 (2019).

20 Ashok A Deniz; Samrat Mukhopadhyay; Edward A Lemke, "Single-molecule biophysics: at the interface of biology, physics and chemistry," Journal of the Royal Society Interface **5** (18) (2007).

21 Hiroyuki Oikawa; Yuta Suzuki; Masataka Saito; Kiyoto Kamagata; Munehito Arai; Satoshi Takahashi, "Microsecond dynamics of an unfolded protein by a line confocal tracking of single molecule fluorescence," Scientific Reports **3** (2013).

22 Kenneth N. Fish, "Total Internal Reflection Fluorescence (TIRF) Microscopy," Curr Protoc Cytom **12** (2009).

23 Andreas S. Biebricher; Iddo Heller; Roel F. H. Roijmans; Tjalle P. Hoekstra; Erwin J. G. Peterman; Gijs J. L. Wuite, "The impact of DNA intercalators on DNA and DNA-processing enzymes elucidated through force-dependent kinetics," Nature Communications **6** (2015).

24 Masoud Karimi Goftar; Nasrollah Moradi Kor; Zahra Moradi Kor, "DNA intercalators and using them as anticancer drugs", (International Journal of Advanced Biological and Biomedical Research, 2014).

25 Brian Herman; Joseph R. Lakowicz; Douglas B. Murphy; Thomas J. Fellers; Michael W. Davidson, "Fluorophores for Confocal Microscopy", (Olympus Corporation), Vol. 2022.

26 "Cyanine Dyes", (Lumiprobe Life Science Solutions).

27 Kenneth R. Spring; Thomas J. Fellers; Michael W. Davidson, "Confocal Microscope Scanning Systems", (Olympus Life Science Solutions), Vol. 2022.

28 Laura M. Higgins; Margot Zevon; Vidya Ganapathy; Yang Sheng; Mei Chee Tan; Richard E. Riman; Charles M. Roth; Prabhas V. Moghe; Mark C. Piercea, "Life-scanning

confocal microscopy for high-resolutino imaging of upconverting rare-earth-based contrast agents," Journal of Biomedical Optics **20** (11) (2015).

29 "How does a confocal microscope work? ".

30 Michael Schriber, "Nobel Prize—Lasers as Tools," Physics **11** (100) (2018);

Thomas J. Fellers; Michael W. Davidson, "Introduction to Confocal Microscopy", (Olympus Life Solutions), Vol. 2022.

31 "C-Trap™ | Product Brochure", (Lumicks).

32 "C-Trap™ G2", (Lumicks).

33 Matthew D Newton; Benjamin J Taylor; Rosalie P C Driessen; Leonie Roos; Nevena Cvetesic; Shenaz Allyjaun; Boris Lenhard; Maria Emanuela Cuomo; David S Rueda, "DNA stretching induces Cas9 off-target activity," Nat Struct Mol Biol **26** (3), 185-192 (2019).

34 Evan Nelsen; Suresh Ramakoti, 2021.

35 B C Delidow; J P Lynch; J J Peluso; B A White, "Polymerase chain reaction: basic protocols," Methods in Molecular Biology **15** (1-29) (1993).

36 SnapGene Software (Insightful Science).

37 J.W. Watters, C-Trap .h5 Visualization GUI (2020).

38 Mario J. Avellaneda; Eline J. Koers; David P. Minde; Vanda Sunderlikova; Sander J. Tans, "Simultaneous sensing and imaging of individual biomolecular complexes enabled by modular DNA–protein coupling," Communications Chemistry **3** (2020).

39 W. S. Rasband, ImageJ, U. S. (National Institutes of Health, Bethesda, MD, USA, 1997-2018).

40 Lumicks, "u-Flux flow cell cleaning protocol," 3 (2022).